**Delineation of Nonrandom Clustering in the Flaking Debris Distribution at 13DB497**

Derek V. Lee[1,2]
[1]*Department of Resource Analysis, Saint Mary's University of Minnesota, Winona, MN 55987*, [2]*Bear Creek Archeology, Inc., Cresco, IA 52136*

*Keywords*: Archeology, Piece-plotting, Late Woodland, Mississippian, Flaking Debris, Nonrandom Clustering

## Abstract

The traditional archeological data recovery method utilizes 1-meter units and screens all matrix through ¼ inch mesh. Modern excavation techniques have begun to incorporate available GIS and survey technology to increase the amount of area surveyed while maintaining more precise provenience information in an effort to interpret community-wide spatial patterns. Typical clustering assessments rely heavily on visual interpretation of point data. However, the level of precision inherent to these datasets enables the quantification and delineation of nonrandom artifact distribution clusters through more statistical means. Flaking debris data from five piece-plotted archeological excavations was compiled to establish sampling accuracy as it pertains to this non-traditional excavation method. Flaking debris from archeological site 13DB497 was selected for in-depth analysis. Statistical procedures were employed to demonstrate both the clustered nature of the distribution as well as to delineate 5 primary clusters. Further interpretations were then conducted to illustrate a potentially significant cultural variation between the 5 clusters and the remaining portion of the excavation.

## Archeological Excavation Methodology

Generally speaking, a traditional archeological mitigation is conducted in one meter units arranged in a fashion sufficient for sampling a defined site area. Typically, units are arranged in a contiguous fashion to form a "trench" or a "block". Their location is generally based on preliminary and/or exploratory test units in an effort to sample the most artifact-laden portion(s) of a site. Each of these units is excavated in levels (e.g. 10 cm) with all associated soil matrix being screened through ¼-inch mesh and recovered artifacts bagged with the

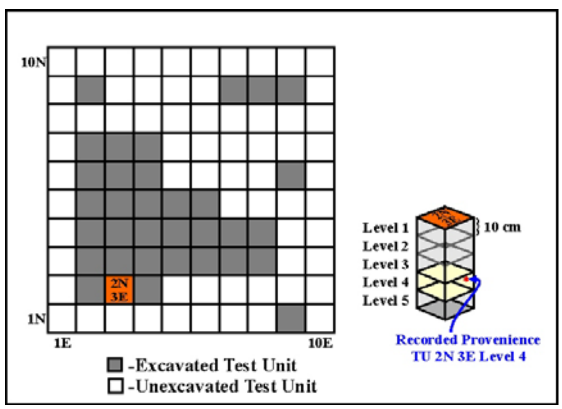


Figure 1. Hypothetical Layout of a traditional excavation.

Lee, Derek. 2006. Delineation of Nonrandom Clustering in the Flaking Debris Distribution at 13DB497. Volume 8, Papers in Resource Analysis. 17 pp. Saint Mary's University of Minnesota Central Services Press. Winona, MN. Retrieved (date) from http://www.gis.smumn.edu/.

corresponding provenience (e.g. TU 2N 3E Level 4). This generally results in artifact provenience information rounded to the nearest meter horizontally and ten centimeters vertically (Figure 1). The one meter unit has been the mainstay of professional archeological field research very nearly since its inception due to the advantages inherent to their convenient dimensions.

The lack of precise provenience information, in conjunction with the inherently discontinuous nature of its sampling through selective bias for artifact-laden areas, tends to exclude subsequently recovered data from in-depth community-wide pattern analysis unless years of field research are conducted. Devoting years of excavation to a single site is cost prohibitive and typically impractical or impossible due to the fact that much fieldwork is now conducted just prior to a site's destruction by impending development. Furthermore, the traditional approach typically samples a very small percent of the site, which suggests the improbability of accurately assessing large-scale community patterns.

The "piece-plotting" method of archeological data recovery developed out of the need to more accurately assess community patterns in order to further the understanding of past cultures through spatial patterning (Benn and Lee 2002; Benn et al. 1999). The technique of precisely mapping artifact locations has been employed since the beginning of modern day archeological science. But, prior to recent technological advances, the process was quite labor intensive and was subsequently reserved for specific circumstances. The past two decades, however, have seen the advent of relatively affordable total station

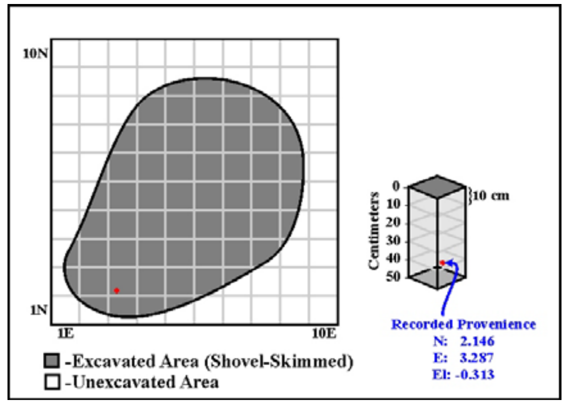

Figure 2. Hypothetical layout of a piece-plotted excavation.

mapping equipment, as well as powerful database and GIS software. These tools enable archeologists to easily and precisely map, track, analyze, and interpret field data.

The piece-plotting method typically involves three steps during excavation: "shovel-skimming" a relatively large area, mapping artifact locations with a total station, and bagging individual artifacts with an assigned point number. Shovel-skimming entails the methodical removal of very thin (<1 cm) layers of soil. Artifacts encountered during this process are left in place and flagged for mapping. The mapping team includes a total station operator and a prism pole operator. Depending on artifact density, a third person may be added strictly to bag artifacts. The pole operator places the prism pole at the artifact location while the total station operator shoots and records a point. During this process, a code number corresponding to a compressed list of artifact categories is relayed to the total station operator and recorded on the data collector. The artifact is placed in a bag that was previously barcoded (pre-field) with the number corresponding to that stored on the data collector. This process results in precise 3-dimensional coordinates

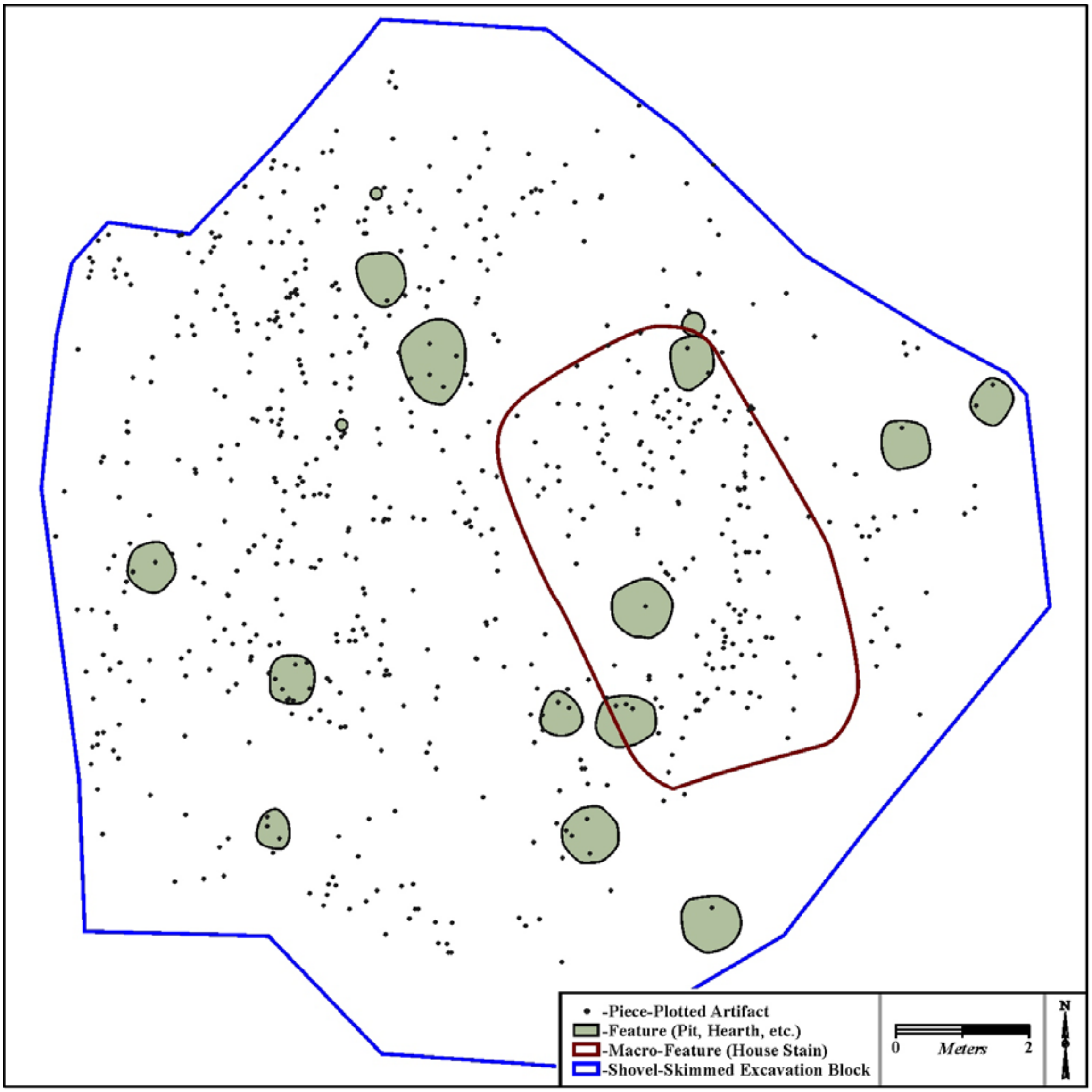

Figure 3. Example of data collected during a piece-plotted excavation (adapted from Benn and Lee 2002).

(e.g. N: 2.146, E: 3.287, El: -0.313) being assigned to individual *in situ* artifacts (Figure 2). The precision of piece-plotted data lends itself to rigorous pattern analysis that is not typically available under traditional field methods.

Data collected using the piece-plotting method consists of three general types: artifacts, features, and macro-features (Figure 3). Artifacts, as described above are point locations representing the occurrence of single artifacts. Features (e.g. hearths, pits, posts, etc.) are mapped and handled separately. When a feature is encountered, an approximate center point is mapped along with endpoints of a bisecting line. Detailed plan and profile sketches are hand drawn and include these three points for post field digitization. Artifacts encountered within the feature are typically collected according to provenience internal to the feature (e.g. Feature 1 N½, Feature 1 Zone 2 W½). Macro-features (e.g. house loci) are areas that typically encompass both piece-plotted artifacts and features. Macro-features are not

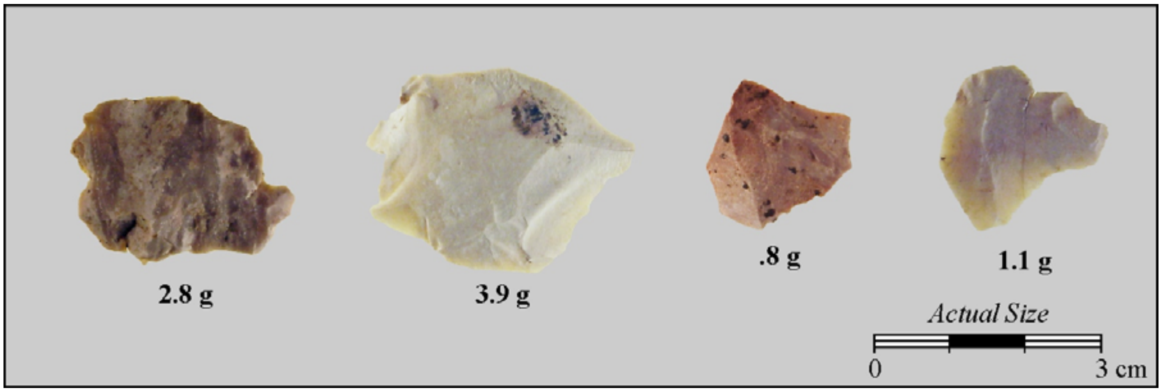

Figure 4. Examples of flaking debris showing respective weights.

always clearly identifiable in the field but their presence/absence can, for the most part, be discerned from distinct feature and artifact distributions (Benn et al. 1999). During excavation, discernable perimeters of macro-features are mapped with missing or inconclusive boundary segments interpolated during post-field data processing.

The primary difference between the traditional and piece-plotting methods relates to the screening of soil matrix through standard-sized mesh. The traditional method processes all excavated material through screens, whereas the piece-plotting method processes but a very small percent of the soil in this fashion. As a result, per hour of labor, a significantly larger area can be excavated using the piece-plotting method. The disadvantage, however, is the inherent loss of smaller artifacts not recovered during the shovel-skimming process. This is compensated for by strategically locating sample areas that are screened, in order to quantify and control for unrecovered artifacts. In-depth artifact distribution analyses and subsequent pattern interpretation of piece-plotted data should acknowledge and control for the potential sample accuracy issues related to artifact recovery.

## Flaking Debris

Flaking debris (Figure 4) is the byproduct of stone tool manufacture and maintenance. Unlike many artifact types (e.g. pottery, cobble tools, chipped stone tools) whose deposition generally occurs at the end of a lengthy use cycle, flaking debris tends to be deposited at its point of origin (Ahler 1989). This is not to say that flakes were not collected and redeposited in a secondary location (e.g. refuse pits), as this undoubtedly occurred and is evidenced in the archeological record. However, flakes recovered from non-feature locations are generally assumed to be in approximately their primary location. The spatial integrity of non-feature flaking debris suggests that they may yield significant information regarding past cultural patterns associated with chipped stone

Table 1. Summary information from the five selected sites.

| Site | Citation | Occupation | Test Units (1 $m^2$) | Excavation Block ($m^2$) | Test Unit Flaking Debris | Excavation Block Flaking Debris |
|---|---|---|---|---|---|---|
| 13AM403 | Benn et al. 2005 | 200 B.C. - A.D. 400 | 5 | 185 | 34 | 448 |
| 13AM404 | Benn et al. 2005 | A.D. 400 - 1200 | 5 | 1,670 | 110 | 4,305 |
| 13DB497 | Benn et al. 2002 | A.D. 1100 | 7 | 835 | 245 | 5,639 |
| 13GT84 | Thompson et al. 2005 | 800 B.C. - 1200 A.D. | 3 | 95 | 34 | 290 |
| 13GT97 | Blikre et al. 2005 | A.D. 400 - 1200 | 5 | 190 | 55 | 827 |

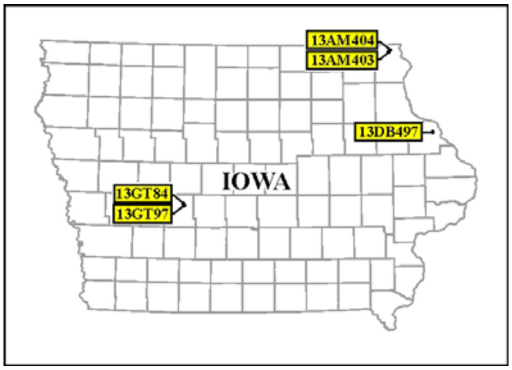

Figure 5. Location of the five selected sites.

tool manufacture and use.

Before an in-depth analysis of flaking debris distribution can be conducted, it is necessary to establish the degree of sampling accuracy inherent to piece-plotted artifacts recovered via shovel-skimming. To address this issue flaking debris data was analyzed from 5 archeological sites (Table 1, Figure 5).

These sites are of varying ages and sizes. Consequently, their respective artifact assemblages range from very small to very large. In the course of mitigation, a number of traditional test units as well as piece-plotted excavation blocks were conducted on each site. The number of traditional test units conducted at each of the five sites was minimal, but the subsequently recovered artifacts are assumed to be representative of the results typical of the traditional method. Data recovered from features (both in

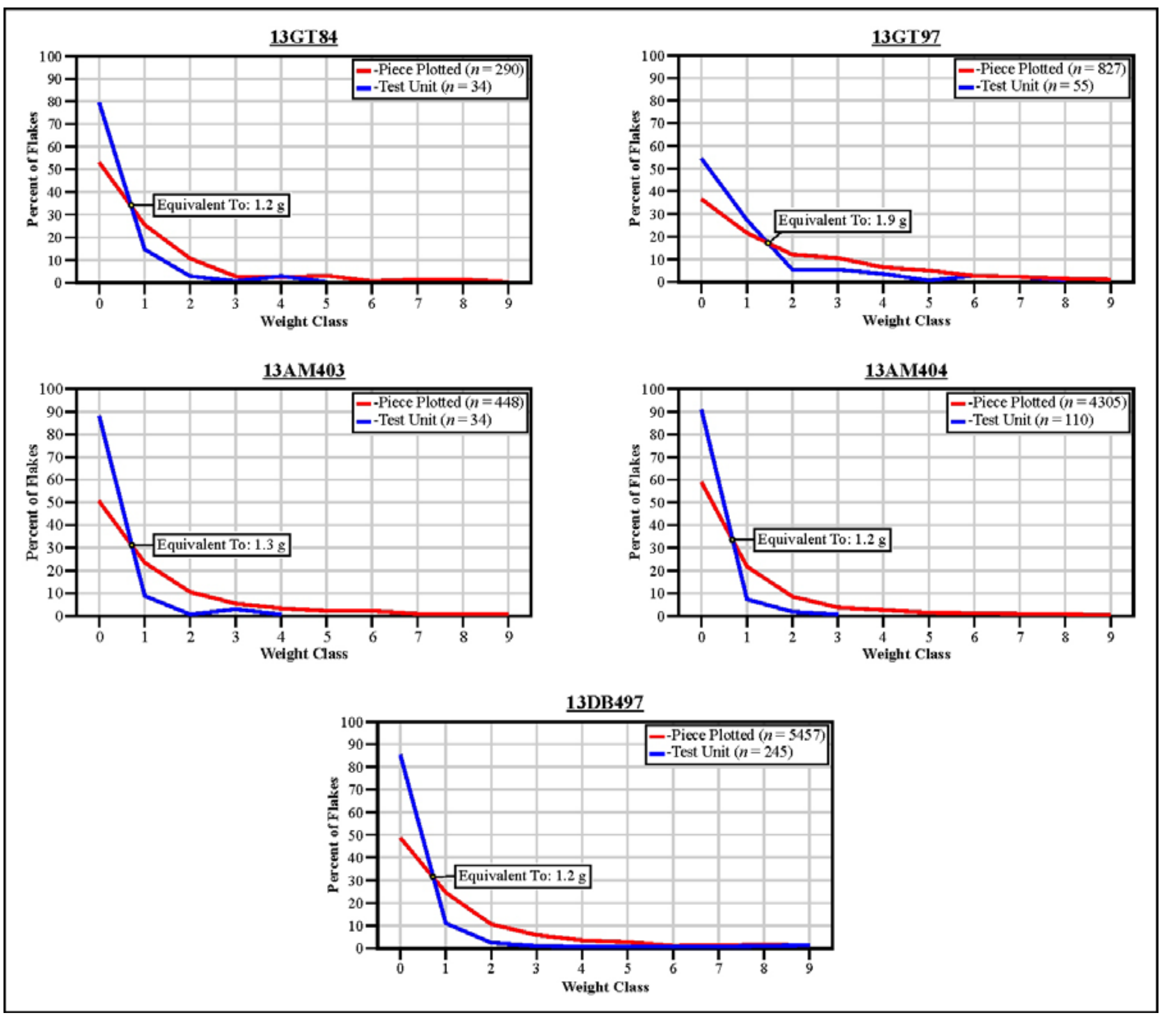

Figure 6. Flaking debris (<10 g) weight class distribution graphs of each site.

test units and piece-plotted blocks) are excluded from this examination since the traditional and piece-plotting methods utilize similar recovery techniques in this respect.

Flake weight was used as an indicator of size, since actual physical dimensions are not typically recorded on a per flake basis. The flaking debris assemblages were limited to flakes weighing less than 10 grams. Flakes weighing more than 10 grams constitute a very small percentage (<1.5%) of the overall sample and their relative size suggests that recovery rates between traditional and piece-plotting methods should be equivalent.

Initially, individual flake weights were classified into 10 categories by truncating weight values at the integer level. Flakes weighing between 0 and .9 grams were classified as 0's, flakes weighing between 1 and 1.9 grams were classified as 1's, and so on. Class ratios were then computed so that the weight distributions could be directly compared. Data from each of the five sites was compiled in this fashion and individually graphed (Figure 6). These indicate that a critical sampling accuracy drop-off point occurs somewhere below 2 grams for the piece-plotted data.

To more accurately determine the critical point, a similar process was conducted for all flakes weighing 2 grams or less. At this stage, data from each of the five sites was compiled into one composite weight distribution curve (Figure 7). This graph indicates the distribution curves are quite similar, especially given the comparatively small size of the test unit collection. Based on this, the under-sampling point appears to be in the vicinity of the .2-.3 gram range. Below 0.2 grams, the tendencies of each curve diverge. Above .3 grams the weight distribution curves approximate each other. The mid-point (.25 grams) of the interval in question was deemed to be as precise an approximation of piece-plotted flaking debris sampling accuracy as possible given standard laboratory procedures that record weight to the nearest .1 gram.

Comparing the piece-plotted flaking debris sampling accuracy of .25 grams to that of the traditional method requires data illustrating a general correlation of flake weight to surface area. To establish this in a preliminary fashion, 150 flakes weighing .3 grams or less were randomly selected. Each was

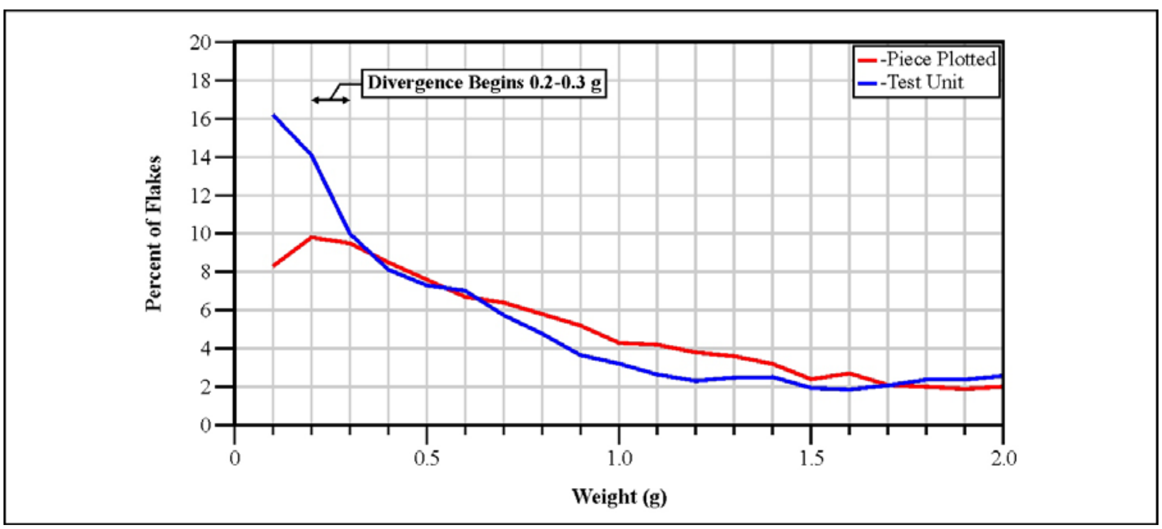

Figure 7. Weight distribution of all flaking debris <2 g.

Table 2. Summary of 150 randomly selected flakes weighing <.3 g.

| Weight (g) | Count | Min. Surface Area (mm²) | Max. Surface Area (mm²) | Mean Surface Area (mm²) |
|---|---|---|---|---|
| .05 | 30 | 20.8 | 26.7 | 24.6 |
| .10 | 21 | 33.1 | 46.2 | 39.2 |
| .15 | 23 | 43.7 | 56.2 | 50.9 |
| .20 | 28 | 54.3 | 64.1 | 60.0 |
| .25 | 26 | 60.2 | 75.3 | 68.6 |
| .30 | 22 | 69.5 | 80.1 | 77.2 |

weighed to the nearest .05 gram and maximum physical dimensions were recorded. The resulting data was then summarized according to weight and surface area (max. length × max. width). These results (Table 2) were then graphed (Figure 8) to illustrate a surface area to weight correlation.

Based on this, the critical sampling accuracy value of .25 grams corresponds to a surface area of 68.6 $mm^2$. Therefore, it is surmised that piece-plotted flaking debris with average physical dimensions below 8.28 mm ($\sqrt{68.6}$ $mm^2$) may not be accurately sampled. The traditional method of data recovery typically screens soil matrix through 6.35 mm (¼-inch) mesh.

These calculations establish a preliminary weight-to-size correlation and provide some insight to the sampling accuracy inherent to the piece-plotting method, however, a great deal more data should be gathered to further refine the approximations used above. Although 150 "random" flakes were used in these calculations it should be noted that the material types included were by chance restricted to fine-grained cherts. Further

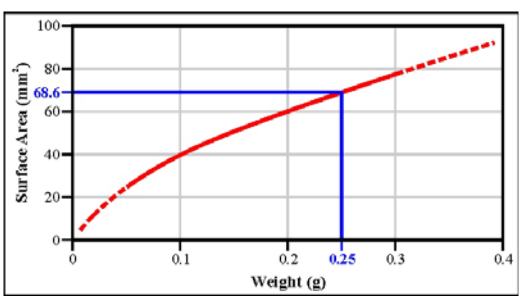


Figure 8. Correlation of flake weight to surface area.

data should be collected to increase sample size and incorporate various material types to improve the accuracy of these results. Furthermore, sampling accuracy and recovery rates may be more dramatically illustrated through direct comparison. Screening measured samples of shovel-skimmed backdirt through traditional ¼-inch mesh and recording surface area dimensions of any recovered artifacts may yield a significantly more detailed understanding of this issue.

**13DB497**

Site 13DB497 (The Union Bench Site) encompasses a palisaded village containing multiple households, a public structure, and a plaza. It was occupied briefly circa A.D. 1100 and represents a mix of terminal Late Woodland and Upper Mississippian peoples (Benn et. al. 2002). Based on the analysis of various artifact types and the distribution patterns of culturally related artifact sub-types, the site demonstrates a striking east-west dichotomy between Late Woodland and Upper Mississippian peoples. The former occupied the western and the latter occupied the eastern portions of 13DB497.

During Phase III data recovery, an excavation block encompassing approximately 835 $m^2$ was shovel-skimmed. A total of 44 cultural features (e.g. hearths, basins, pits) and 11 structure loci (macro-features) were documented in the excavation block. A total of 14,158 artifacts were recovered during the excavation, of which 8,968 (63%) were piece-plotted and 5,190 (37%) were from features. Of the piece-plotted artifacts, 5,639 (63%) are flaking debris (Table 3). The distribution of artifacts, features, and macro-features is

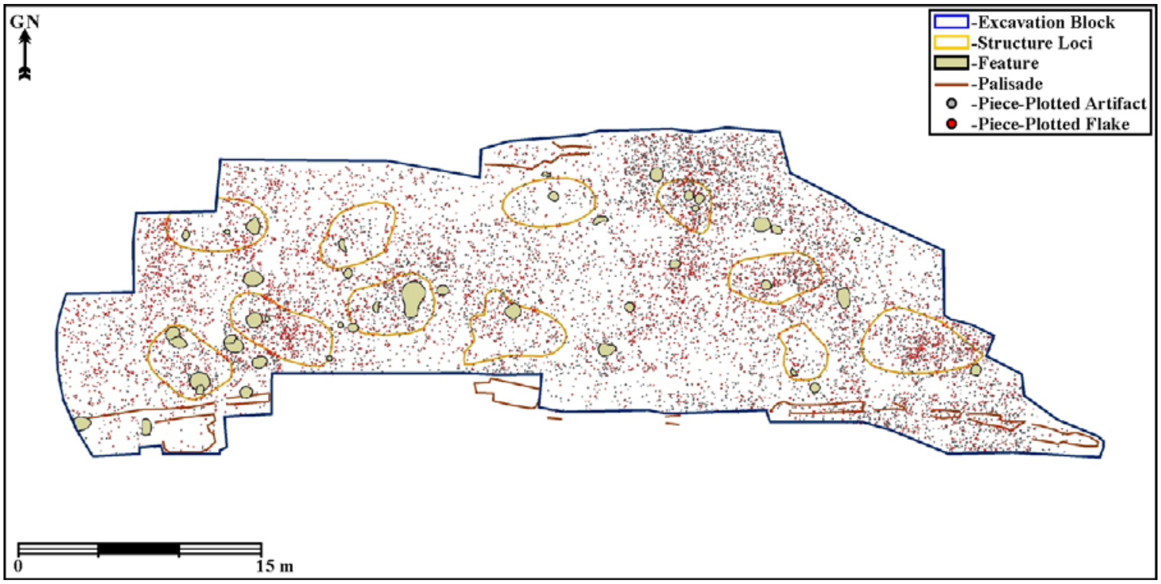

Figure 9. Distribution of artifacts, features, and macro-features at 13DB497.

illustrated in Figure 9. As flaking debris constitutes the majority of piece-plotted artifacts at 13DB497, their distribution should be of particular interest.

Correcting the 13DB497 flaking debris data set for the sampling accuracy rate calculated above, involves removing flakes weighing less than .25 grams from the population. Of the 5,639 piece-plotted flakes, 726 (13%) fall into this category. The remaining 4,913 (87%) are deemed to accurately represent the flaking debris population weighing more than .25 grams (Figure 10). The 726 flakes removed from the population *may* be a representative sample of flakes weighing less than .25 grams, however, the potential for sampling inaccuracies could result in misguided cluster delineations. Further analysis of the distribution of these flakes could be conducted to gauge the significance of this assumption.

Table 3. Summary of 13DB497 piece-plots.

| Category | Count | Percent |
|---|---|---|
| Burned Earth | 29 | 0.32 |
| Charcoal | 7 | 0.08 |
| Cobble Tool | 15 | 0.17 |
| Core | 109 | 1.22 |
| Chipped Stone Tool | 435 | 4.85 |
| Fire-Cracked Rock | 1,477 | 16.47 |
| Flaking Debris | 5,639 | 62.88 |
| Groundstone Tool | 7 | 0.08 |
| Hematite | 2 | 0.02 |
| Historic | 98 | 1.09 |
| Introduced Rock | 248 | 2.77 |
| Lead | 18 | 0.20 |
| Modified Bone | 11 | 0.12 |
| Pottery | 723 | 8.06 |
| Unmodified Bone | 150 | 1.67 |
| **Total** | **8,968** | **100.00** |

To assess the distribution of the remaining 4,913 flakes with regards to their state of randomness, a 50 cm grid shapefile was generated from an exported Microsoft Access table of incremented 50 cm point coordinates spanning the extents of the excavation block. The Edit Tools extension for ESRI's ArcView was used to "connect" these points and generate a shapefile of adjoining 50 cm squares (Figure 11). A union was then performed on the excavation block and 50 cm grid. The resulting shapefile was trimmed to include only the grid portion internal to the excavation block (Figure 12). Next, a union was performed on the grid layer and the feature layer, which was similarly trimmed to exclude feature related grid cells. Finally, cells with a surface area less than .238 $m^2$ (95% of a

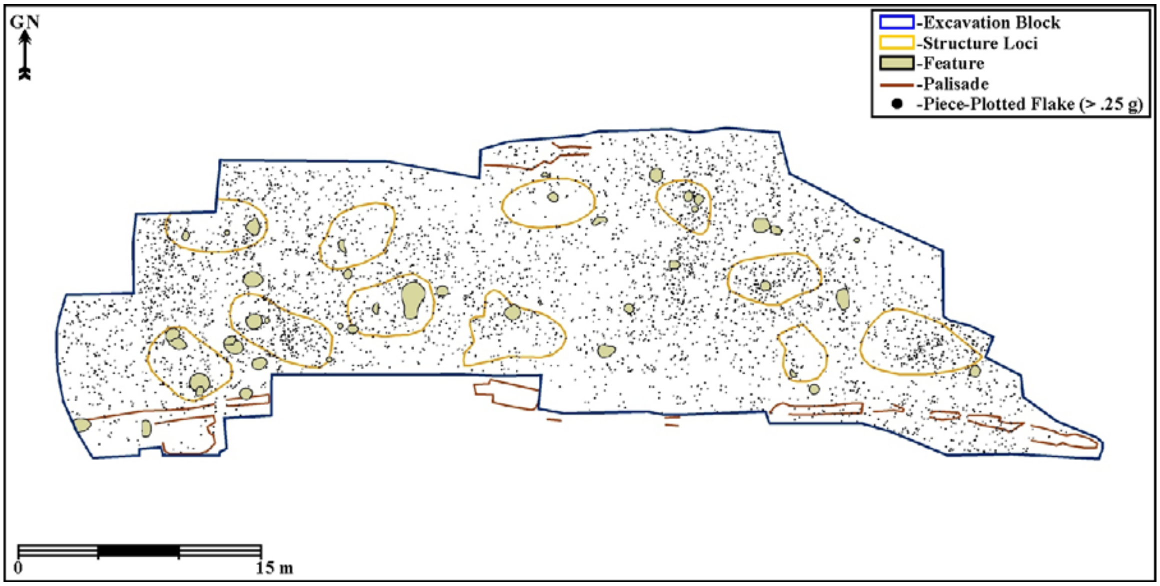

Figure 10. Distribution of piece-plotted flakes weighing more than .25 g.

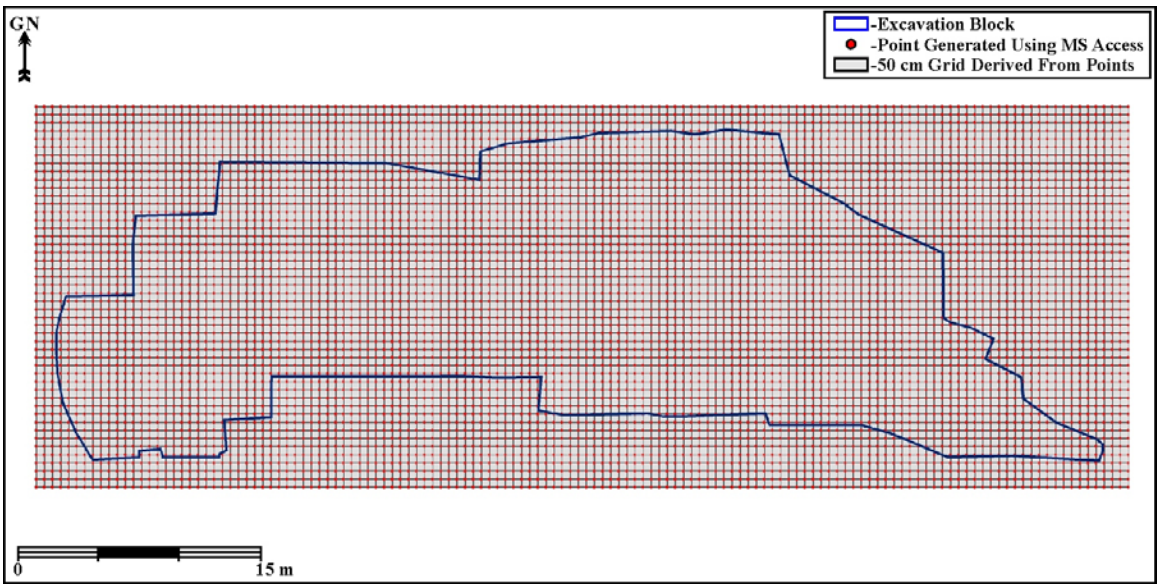

Figure 11. The 50 cm grid shapefile generated using MS Access and the Edit Tools extension.

50 cm × 50 cm cell) were removed from the set. This resulted in a 50 cm grid across the block excluding feature related cells and fractional squares along the boundary of the excavation (Figure 13). The final 50 cm grid shapefile contained a total of 3,028 individual cells with an average area of .2499 $m^2$ per cell and covered a total of 756.7 $m^2$.

Individual flakes in the corrected flaking debris distribution (Figure 10) were assigned the cell ID value corresponding to the 50 cm grid cell in which it resided. This was done via the spatial join feature of ArcView. The resulting table was summarized to produce a table of cell IDs and their respective total flake counts. This table was then joined to the original grid table via the ID field, and exported as another theme. The result was a 50 cm grid across the excavation block with a total flake count for each cell (Figure 14).

Figure 12. The 50 cm grid trimmed to the excavation block showing the location of features.

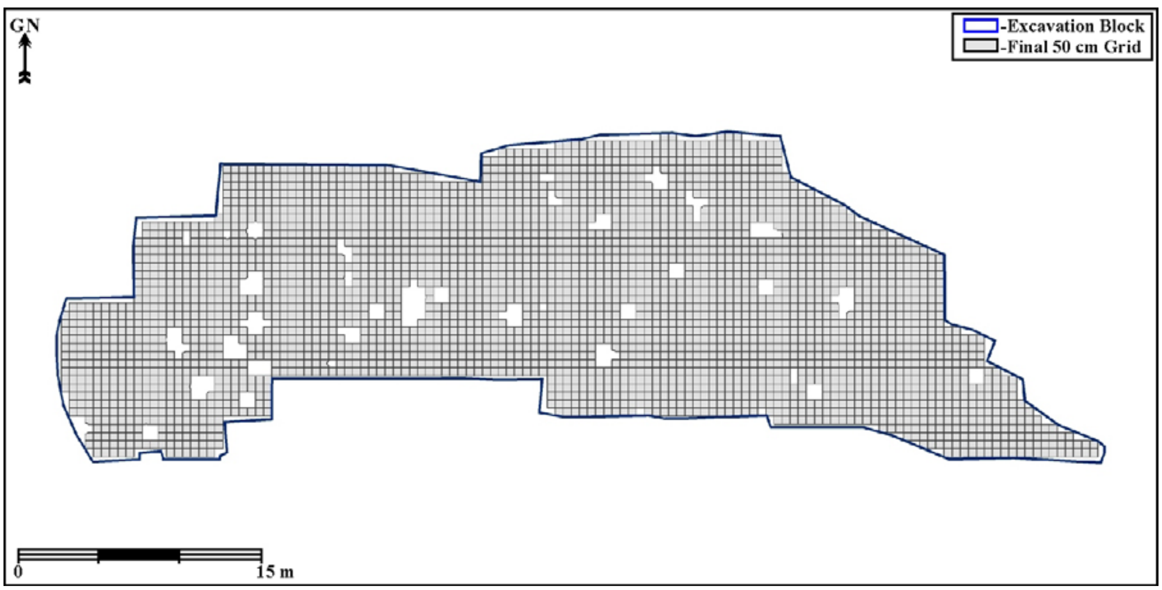

Figure 13. The final version of the 50 cm grid shapefile.

Of the 4,913 flakes in the corrected data set, 4,531 (92%) fell into one of the 50 cm cells. The remaining 382 (8%) fell outside of the grid, either near the excavation perimeter or near a feature.

A visual assessment of Figure 14 suggests possible clustering in the distribution of flaking debris. To address this observation in a more statistical fashion, a Poisson distribution goodness of fit test (Zar 1999) was conducted on the hypotheses:

$H_0$: Flaking debris is distributed randomly in the excavation block.
$H_A$: Flaking debris is not distributed randomly in the excavation block.

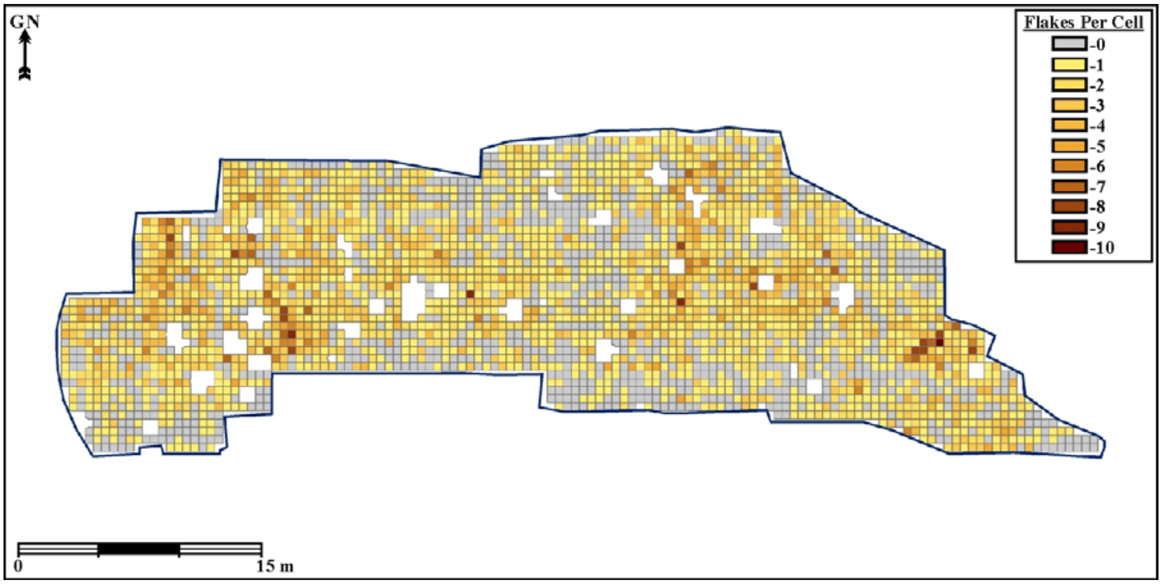

Figure 14. Flake counts per 50 cm cell.

In Table 4, $X_i$ is the number of flakes in a 50 cm cell, $f_i$ is the number of cells having the corresponding $X_i$ flakes, $P(X_i)$ is the statistical probability of having $X_i$ flakes in a given 50 cm cell, $[P(X_i)][n]$ represents the number of flakes expected to be observed in cells having $X_i$ flakes in a random distribution.

Since $H_0$ must be rejected, the alternate hypothesis is accepted. Based on the Poisson distribution goodness of fit test conducted above, it can be concluded that the flaking debris distribution in the excavation block at 13DB497 is *not* random.

Summarizing the table associated with the flaking debris distribution grid finds that the dataset has a mean (μ) of 1.4964 flakes per cell with a corresponding variance ($\sigma^2$) of 2.3187. Since $\sigma^2 > \mu$, it can further be concluded that the distribution is clustered. As a test of the statistical significance of this conclusion, a Visual Basic for Applications (VBA) script was written to randomly distribute the same number of flakes ($n$=4,531) among the 3,028 grid cells. To accomplish this task, the table associated with the 50 cm grid shapefile was exported as a text file. A Microsoft Access database was created and the text file was imported as a new table. A new integer field, RandomCount, was added to the table design. The script (Figure 15) was then written under the “OnClick” event procedure of a button on a new form.

Table 4. Poisson distribution statistics.

| $X_i$ | $f_i$ | $f_iX_i$ | $P(X_i)$ | $[P(X_i)][n]$ | $\chi^2$ |
|---|---|---|---|---|---|
| 0 | 928 | 0 | 0.224 | 678.346 | 91.881 |
| 1 | 861 | 861 | 0.335 | 1,014.806 | 23.311 |
| 2 | 605 | 1,210 | 0.251 | 759.075 | 31.274 |
| 3 | 331 | 993 | 0.125 | 378.525 | 5.967 |
| 4 | 167 | 668 | 0.047 | 141.568 | 4.569 |
| 5 | 69 | 345 | 0.014 | 42.357 | 16.758 |
| 6 | 36 | 216 | 0.003 | 10.561 | 61.276 |
| 7 | 15 | 105 | 0.001 | 2.257 | 71.945 |
| 8 | 12 | 96 | 0.000 | 0.422 | 317.598 |
| 9 | 3 | 27 | 0.000 | 0.070 | 122.353 |
| 10 | 1 | 10 | 0.000 | 0.010 | 93.289 |
| | **3,028** | **4,531** | **1.000** | **3,027.998** | **840.221** |

$$n = \sum f_i = 3028$$

$$\mu = \frac{\sum f_i X_i}{\sum f_i} = \frac{4531}{3028} = 1.4964$$

$$v = 11 - 2 = 9$$

$$\chi^2_{0.01,9} = 21.666$$

Since 21.666 < 840.221, Reject $H_0$

The script initially passes through the grid table and sets the RandomCount field to 0. Then it conducts 4,531 iterations of randomly selecting a number between 1 and 3,028 (inclusive), and adding 1 to the RandomCount field of the 50 cm cell with the ID field corresponding to the randomly selected number. This results in 4,531 hypothetical flakes randomly assigned to one of the 3,028 valid 50 cm cells. Next the script calculates the mean (always 4,531/3,028 or 1.4964) and variance of the randomly distributed hypothetical flakes and writes those values to a new record in a separate table named “RandomResults”. This process was than iterated 5,000 times to gauge

```
Dim T As Recordset
Dim RR As Recordset
Dim Q1 As Recordset

Dim N As Integer
Dim Z As Integer
Dim R As Integer
Dim SS As String
Dim SQL1 As String

Set RR = CurrentDb.OpenRecordset("RandomResults", dbOpenDynaset)

'ESTABLISH SQL STATEMENT FOR MEAN AND VARIANCE
SQL1 = "SELECT Blocks_50cm.Per, Sum(Blocks_50cm.RandomCount) AS Count,_
        Avg(Blocks_50cm.RandomCount) AS Mean, Var(Blocks_50cm.RandomCount) AS Variance_
        FROM Blocks_50cm GROUP BY Blocks_50cm.Per;"

For Z = 1 To 5000     'ITERATIONS TO RUN

  'SET RANDOM COUNT FIELD TO ZERO
  Set T = CurrentDb.OpenRecordset("Blocks_50cm", dbOpenDynaset)
  T.MoveFirst
    Do Until T.EOF
      T.Edit
      T![RandomCount] = 0
      T.Update
    T.MoveNext
    Loop
  T.Close

  'RANDOMLY DISTRIBUTE EQUIVALENT NUMBER OF FLAKES
  Set T = CurrentDb.OpenRecordset("Blocks_50cm", dbOpenDynaset)
  For N = 1 To 4531           'NUMBER OF FLAKES = 4531
    R = Int((3028 * Rnd) + 1)    'NUMBER OF 50cm BLOCKS = 3028
    SS = "[ID] = " & R
    T.FindFirst SS
    If Not T.NoMatch Then        'FIND MATCHING SEQUENTIAL 50 cm CELL ID
      T.Edit
      T![RandomCount] = T![RandomCount] + 1   'ADD 1 TO THE RANDOM COUNT FIELD
      T.Update
    End If
  Next N
  T.Close

  Set Q1 = CurrentDb.OpenRecordset(SQL1, dbOpenDynaset)  'LOAD SUMMARY STATISTICS
  Q1.MoveFirst
    RR.AddNew
    RR![Count] = Q1![Count]
    RR![MEAN] = Q1![MEAN]
    RR![VARIANCE] = Q1![VARIANCE]
    RR.Update
  Q1.Close


Next Z

MsgBox "Complete..."
```

Figure 15. VBA script used to randomly distribute flakes among cells.

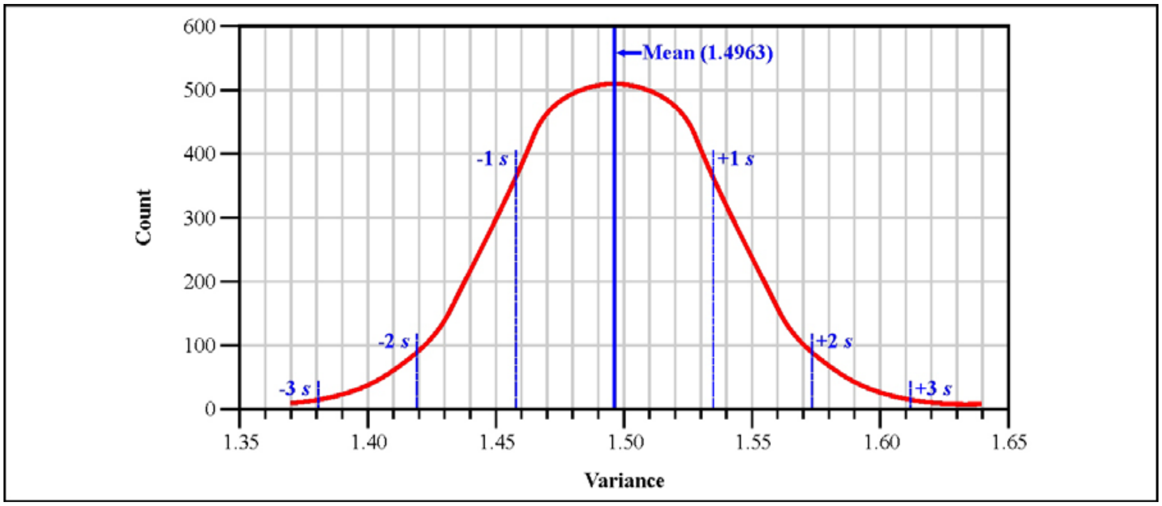

Figure 16. Variance summary of 5,000 iterations.

precisely how much variance could be expected in a random distribution given a reasonable degree of probability.

The resulting list of 5,000 means and variances were than summarized (by rounding to the second decimal) and graphed to show the expected normal distribution curve (Figure 16). A standard deviation of .0385 was calculated from these values. This suggests that, even given three standard deviations (approximately 99%) above and below the mean of 1.4964, the variance of a random flake distribution will be between 1.3809 and 1.6119. Therefore the observed variance of 2.3817 suggests the flake distribution at 13DB497 is clustered beyond any reasonably likely random occurrence.

Given the above calculation results it is now possible to analyze the 13DB497 flake distribution for concentrations that exceed random likelihood. Using the values calculated in Table 4 it is noted that the cells having 4 or more flakes should comprise 6.5% of the flakes (approximately 295) if the distribution were random.

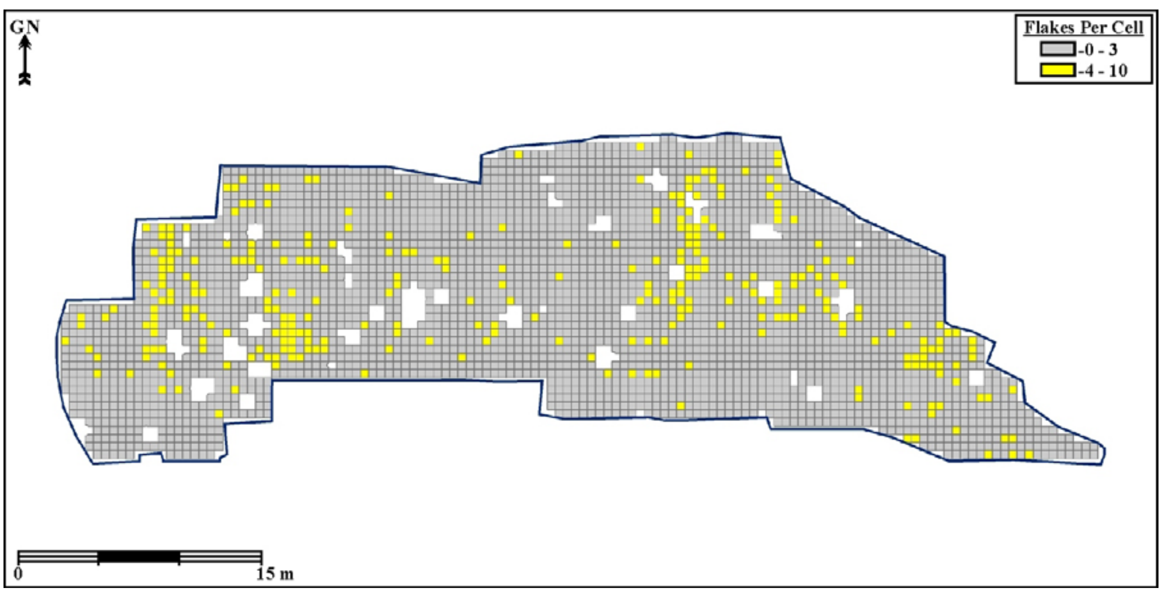

Figure 17. Distribution of cells having 4 or more flakes.

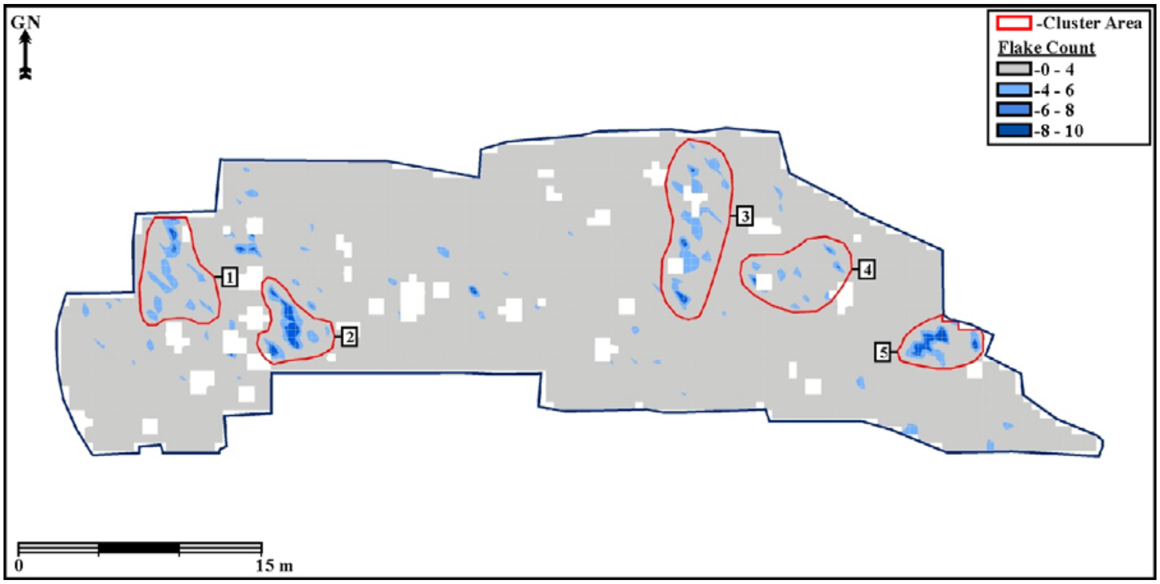

Figure 18. Delineated cluster areas overlain on TIN.

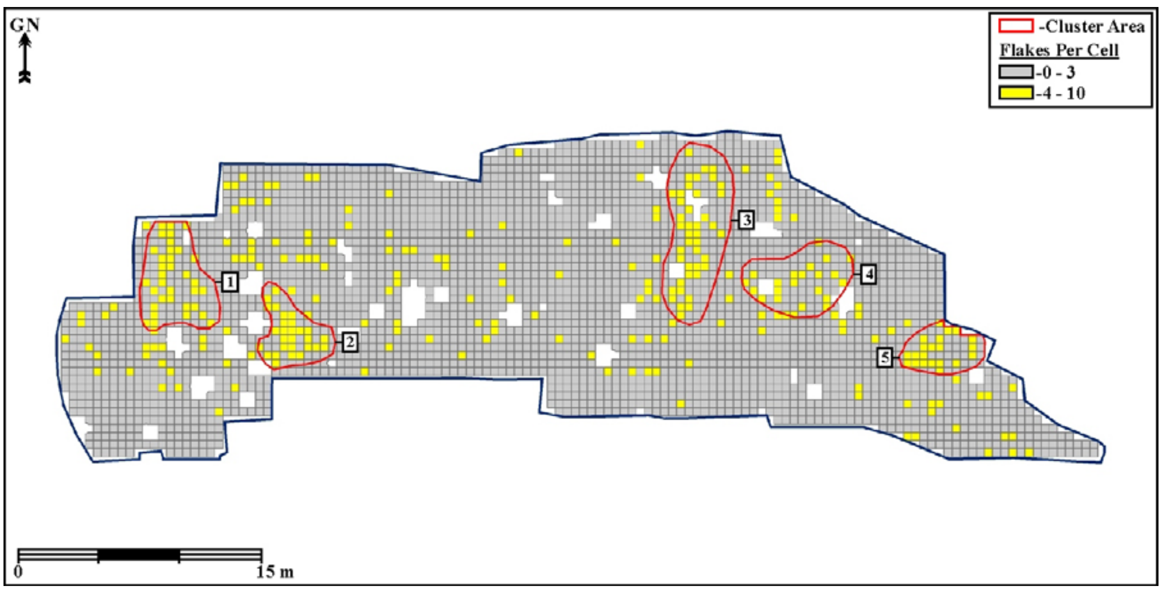

Figure 19. Delineated cluster areas and concentrated cells.

However, the actual observed frequency of $f_4X_4 + f_5X_5 + \ldots + f_{10}X_{10}$ equates to 1,467 flakes or 32%. Furthermore, the number of cells having 4 or more flakes, $f_4 + f_5 + \ldots + f_{10}$, equals 303 or approximately 10%. In other words, 10% of the cells contain 32% of the flakes versus the random expectation of 6.5%. The distribution of this is shown in Figure 17.

A TIN surface was generated from the 50 cm grid shapefile values to further enhance the visualization of flaking debris concentrations by softening the 50 cm cell boundaries through incorporation of data from adjoining cells. It should be noted that the distribution of the more concentrated cells tend to cluster toward 5 primary and discrete locations (Figure 18).

Next, the 50 cm grid shapefile was dissolved based on a generic field set to 0 for each cell. The resulting shapefile represents the boundary of the

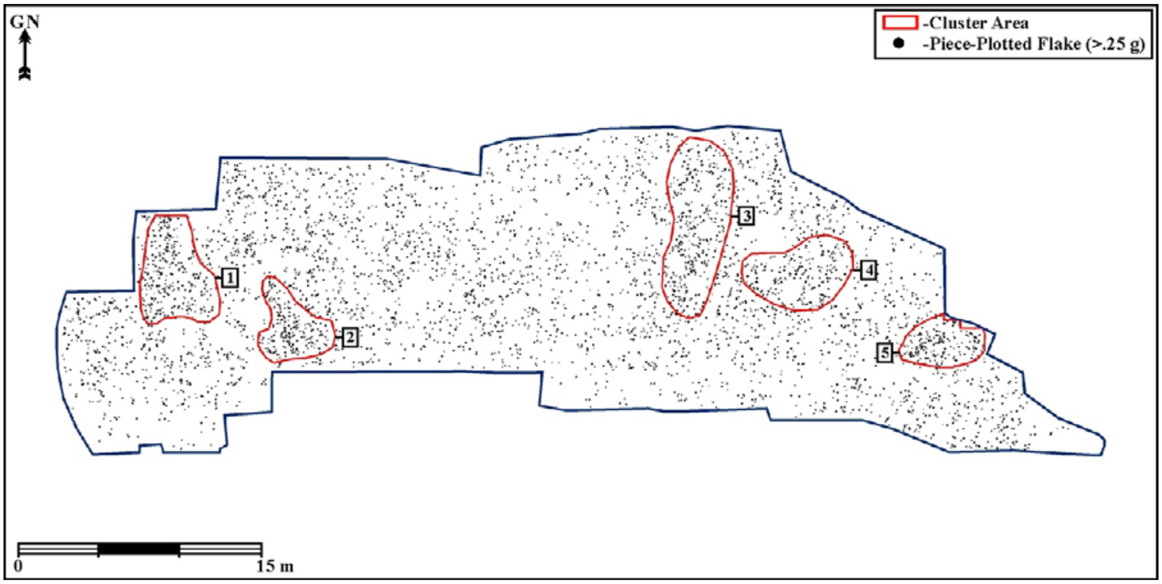

Figure 20. Delineated cluster areas and piece-plotted flakes within the 50 cm grid.

original 50 cm grid. This boundary was then unioned with the shapefile of concentration areas. The result, after eliminating sliver shapes around feature exclusions is a shapefile delineating 5 cluster areas and the boundary of the entire 50 cm grid. A new field, "Area", was added to the underlying table and each shape's surface area was calculated using the field calculator feature of ArcView. Summarizing this table indicates the clusters comprise 105.8 $m^2$ versus the non-cluster area of 650.9 $m^2$.

Of the 303 cells having flake counts of 4 or more, 151 (50%) lie in the 5 delineated clusters (Figure 19). Based on the combined areas of the 5 clusters (105.8 $m^2$ or 14%) versus the remaining portion of the 50 cm grid (650.9 $m^2$ or 86%) one would expect approximately 42 cells (14% of 303) to contain 4 or more flakes in the cluster areas if the concentrated cells were themselves randomly distributed. The fact that 151, or 360% of the expected 42, lie within the 5 clusters further indicates the significance of this delineation.

It is now possible to analyze the distribution for variations between concentration areas and non-concentration areas using the previously established cluster boundaries. A spatial join was preformed on the flaking debris point shapefile to assign each flake its respective area designation (Figure 20). Next, the table was exported from ArcView and imported into a Microsoft Access database for further processing. At this point, flakes weighing over 10 grams were eliminated from the dataset due to their statistically overwhelming weight disparity and the subsequent tendency to skew weight distribution interpretation. Of the 4,538 flakes, 162 (3.6%) weighed more than 10 grams, leaving 4,376 (96.4%) flakes in the data set. These have a mean weight of 1.86 grams as illustrated in Figure 21.

A crosstab query was then generated to calculate the mean weight of flakes by concentration versus non-concentration area. The results of the query indicate virtually no disparity in the relative weight of flakes between the clustered areas ($\bar{X}$ = 1.90) and the non-clustered area ($\bar{X}$ = 1.84). The crosstab query was then modified to summarize the individual concentration areas and the non-concentration area. This results in the observation that Cluster Areas 1

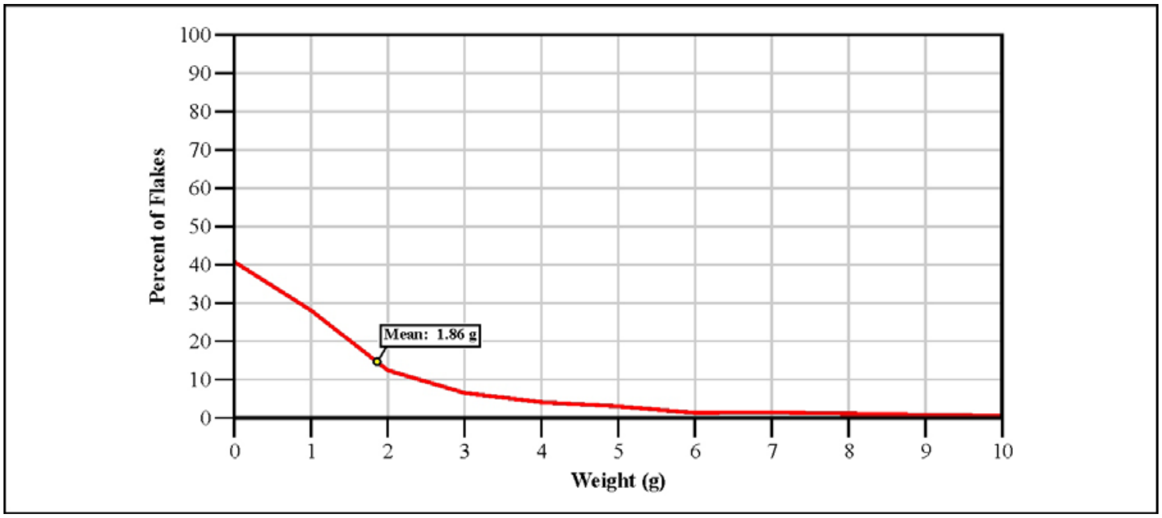

Figure 21. Weight distribution of piece-plotted flakes (≤10 g) in the 50 cm grid.

($\bar{X}$ = 1.70) and 2 ($\bar{X}$ = 1.42) have mean flake weights smaller than the overall dataset ($\bar{X}$ = 1.86). Cluster Areas 3 ($\bar{X}$ = 2.13), 4 ($\bar{X}$ = 2.22), and 5 ($\bar{X}$ = 2.03) have mean flake weights greater than expected. The remaining non-concentrated area ($\bar{X}$ = 1.84) very closely resembles the overall dataset. This observation may have cultural implications due to the aforementioned Late Woodland (Cluster Areas 1 and 2) and Mississippian (Cluster Areas 3, 4, and 5) dichotomy present at 13DB497. Further analysis would need to be conducted in order to determine what chipped stone tool manufacture/maintenance differences may account for the disparity.

## Conclusions

This analysis has preliminarily illustrated the extent to which smaller artifact types, particularly flaking debris, may be underrepresented in artifact assemblages acquired via the piece-plotting excavation method. Quantification of this sampling discrepancy should overcome most sampling concerns related to not screening soil matrix through traditional ¼-inch mesh. The in depth analysis of piece-plotted flaking debris from archeological site 13DB497 demonstrates a method for delineating artifact clusters that exceed random chance. Five such clusters were identified in this fashion. Analysis of the cluster areas demonstrated a measurable difference in mean flake weights between the previously identified Late Woodland and Mississippian portions of the site. Further research incorporating data from the distribution of chipped stone tools would be required to postulate plausible inferences about cultural differences in stone tool manufacture and use patterns between the two groups.

## Acknowledgements

I wish to thank Bear Creek Archeology, Inc. of Cresco, Iowa for allowing access to the data sets used in this paper. And to its staff (particularly David Stanley, David Benn, Joe Thompson, and Lowell Blikre) for their insights and comments. Also, I wish to sincerely thank Dr. David McConville of Saint Mary’s University of Minnesota, whose instruction over the years has been profoundly appreciated.

Also, to the many agencies who have funded the archeological mitigations discussed in this text including: U.S. Army Corps of Engineers Rock Island District, Iowa Department of Transportation, Office of the Allamakee County Engineer, and the Lake Panorama Association.

**References**

Ahler, S.A. 1989. Mass Analysis of Flaking Debris: Studying the Forest Rather Than the Tree. Archeological Papers of the American Anthropological Association 1:85-118.

Benn, D.W., E.A. Bettis, W.T. Billeck, L.R. Blikre, L.E. Burgess, L.S. Kelly, G.S. Powell, J.R. Straka, J.B. Thompson, R.C. Vogel, and D.V. Lee 2005. The Hartley Bridge Project Excavations at the Wilde Sites 13AM403, 13AM404, 13AM405, Allamakee County, Iowa. Report #956. Bear Creek Archeology, Inc. Cresco, IA.

Benn, D.W., and D.V. Lee 2002. A Late Woodland Louisa Phase Household in the Upper Mississippi Valley, Henderson County, Illinois. Illinois Archaeology, 14:1-40.

Benn, D.W., J.B. Thompson, D.V. Lee 1999. Prehistoric Households in Iowa. The Wisconsin Archeologist 80:161-210.

Benn, D.W., G.S. Powell, E.A. Bettis, W. Isenberger, D.V. Lee 2002. Data Recovery Excavations at the Terminal Late Woodland Period Union Bench Site (13DB497), Dubuque County, Iowa. Report #847. Bear Creek Archeology, Inc. Cresco, IA.

Blikre, L.R., D.W. Benn, and D.V. Lee 2005. Phase II Archeological Site Testing at 13GT109 and Phase III Archeological Data Recovery at 13GT97 in Victory Township, Guthrie County, Iowa. Report #1224. Bear Creek Archeology, Inc. Cresco, IA.

Thompson, J.B., D.W. Benn, L.R. Blikre, A.J. Hoppin, and D.V. Lee 2005. Phase II Archeological Testing of Five Prehistoric Sites and Phase III Data Recovery on 13GT84, 13GT88, and 13GT90, Lake Panorama, Guthrie County, Iowa. Report #1212. Bear Creek Archeology, Inc. Cresco, IA.

Zar, J.H. 1999. Biostatistical Analysis. Prentice Hall, Upper Saddle River, New Jersey.